

Influences of Radiation Pressures on Mass Estimates of Supermassive Black Holes in AGNs

H. T. Liu^{1,2}, H. C. Feng^{1,3} and J. M. Bai^{1,2}

htliu@ynao.ac.cn

Received _____; accepted _____

¹Yunnan Observatories, Chinese Academy of Sciences, Kunming, Yunnan 650011, China

²Key Laboratory for the Structure and Evolution of Celestial Objects, Chinese Academy of Sciences, Kunming, Yunnan 650011, China

³University of Chinese Academy of Sciences, Beijing 100049, China

ABSTRACT

In this paper, we investigate the influences of two continuum radiation pressures of the central engines on the black hole mass estimates for 40 active galactic nuclei (AGNs) with high accretion rates. The continuum radiation pressure forces, usually believed negligible or not considered, are from two sources: the free electron Thomson scattering, and the recombination and re-ionization of hydrogen ions that continue to absorb ionizing photons to compensate for the recombination. The masses counteracted by the two radiation pressures M_{RP} depend sensitively on the percent of ionized hydrogen in the clouds β , and are not ignorable compared to the black hole virial masses M_{RM} , estimated from the reverberation mapping method, for these AGNs. As β increases, M_{RP} also does. The black hole masses M_{\bullet} could be underestimated at least by a factor of 30–40 percent for some AGNs accreting around the Eddington limit, regardless of redshifts of sources z . Some AGNs at $z < 0.3$ and quasars at $z \gtrsim 6.0$ have the same behaviors in the plots of M_{RP} versus M_{RM} . The complete radiation pressures will be added as AGNs match $M_{\text{RP}} \gtrsim 0.3M_{\text{RM}}$ due to the two continuum radiation pressures. Compared to M_{RM} , M_{\bullet} might be extremely underestimated if considering the complete radiation pressures for the AGNs accreting around the Eddington limit.

Subject headings: galaxies: active – galaxies: nuclei – galaxies: Seyfert – quasars: general – quasars: supermassive black holes

1. INTRODUCTION

Active galactic nuclei (AGNs), such as quasars and Seyfert galaxies, are powered by gravitational accretion of matter onto supermassive black holes in the central engines. The energy conversion in AGNs is more efficient as implied by high flux variability and short variability timescales (Ulrich et al. 1997). Accretion of matter onto black holes can have high energy release efficiency (Rees et al. 1982; Rees 1984). Broad-line regions (BLRs) in AGNs are photoionized by the central radiation of accretion disks. The broad emission line variations will follow the ionizing continuum variations due to the photoionization process (e.g. Blandford & McKee 1982; Peterson 1993). The reverberation mapping model was tested with the reverberation mapping observations (e.g. Kaspi & Netzer 1999; Kaspi et al. 2000; Peterson et al. 2005). A review about the reverberation mapping research studies is given by Gaskell (2009, and references therein). A general assumption for the cloud ensemble is often virial equilibrium. The BLRs are mainly dominated by the gravitational potentials of the supermassive black holes. This would imply Keplerian orbits of clouds, and this was supported with evidence for the Keplerian motions of the BLR clouds within the well-studied Seyfert 1 galaxy NGC 5548 (e.g. Peterson & Wandel 1999; Bentz et al. 2007). The virialization assumption has been commonly and widely accepted for the reverberation mapping observations to estimate the black hole masses M_{\bullet} . This treatment neglects the contribution of a radiation pressure to the dynamics of clouds.

As the central ionizing source is photoionizing the BLR clouds, the central radiation will produce a radiation pressure on the clouds. The radiation pressure will counteract a part of the gravitational force of a black hole. Thus, the clouds undergo a decrease of the effective gravity of the black hole, and then the orbital velocities of the clouds will decrease for the same orbital radii. In general, this will decrease the widths of broad emission lines, and then lead to underestimate the black hole masses based on the

reverberation mapping method. The radiation pressure force may contribute significantly to the cloud motion, and in this case the clouds on bound orbits could be significantly sub-Keplerian (Marconi et al. 2008, 2009; Netzer 2009; Netzer & Marziani 2010; Krause et al. 2011). However, most of the photoionized gas in the BLR follows Keplerian orbits (Baskin et al. 2014). Marconi et al. (2008) studied the effect of radiation pressure on black hole virial mass estimates for narrow-line Seyfert 1 galaxies, and the black hole virial masses might be significantly underestimated if the radiation pressure is neglected. Netzer (2009) found that the radiation pressure force is not important in $0.1 \leq z \leq 0.2$ AGNs with $L(5100\text{\AA}) = 10^{42.8-44.8} \text{ erg s}^{-1}$. The simple virial mass estimates can give a reasonable approximation to M_{\bullet} even when the radiation pressure force is important (Netzer & Marziani 2010). In the reverberation mapping researches (e.g. Kaspi & Netzer 1999; Kaspi et al. 2000; Peterson et al. 2005), the radiation pressures of the central engines were not considered in estimating M_{\bullet} for the broad-line AGNs. The continuum radiation pressures due to the free electron Thomson scattering and the recombination and re-ionization of hydrogen ions are usually believed negligible or not considered. In this paper, we will investigate the influences of the continuum radiation pressures on the black hole mass estimates for AGNs with high accretion rates, including quasars and broad-line Seyfert 1 galaxies.

The structure of this paper is as follows. Section 2 presents model. Section 3 presents applications. Section 4 is for discussion and conclusions. In this work, we assume the standard Λ CDM cosmology with $H_0 = 70 \text{ km s}^{-1} \text{ Mpc}^{-1}$, $\Omega_M = 0.30$, and $\Omega_{\Lambda} = 0.70$.

2. MODEL

Several assumptions are made. First, the clouds mainly consist of hydrogen and are partially ionized. Second, the clouds are blobs at the distance R from the central black hole.

Dynamical equilibrium corresponds to circular orbits (e.g. Krause et al. 2011). Third, the clouds are in the circular orbits. Fourth, the clouds are optically thin to the Thomson scattering. A cloud has a mass $m \approx Nm_{\text{H}}$, where N is the total number of hydrogen in the cloud and m_{H} is the mass of hydrogen atom. The cloud is subject to the gravity of the central black hole with a mass M_{\bullet} , and the gravity F_{G} is

$$F_{\text{G}} = \frac{GM_{\bullet}m}{R^2}, \quad (1)$$

where G is the gravitational constant, and R is the orbital radius of this cloud. The cloud is exerted with a centrifugal force F_{c}

$$F_{\text{c}} = \frac{mv^2}{R}, \quad (2)$$

where v is the circular velocity. Here, we consider two origins of continuum radiation pressure forces on a cloud: the Thomson scattering of the central source radiation by free electrons, and the recombination and re-ionization of hydrogen ions that will continue to absorb ionizing photons to compensate for the recombination. The recombination line photon number per unit time, i.e., the recombination rate of the ionized hydrogen, is $v_{\text{rec}} = n_{\text{e}}N_{\text{H}^+}\alpha_{\text{B}} = \beta N n_{\text{e}}\alpha_{\text{B}}$, where α_{B} is the hydrogen recombination coefficient, n_{e} is the number density of the free electrons, β is within $0 \leq \beta \leq 1$, and N_{H^+} is the number of the hydrogen ions. On the hydrogen ionizing timescale τ_{ion} , the neutral hydrogen atoms from the recombination are re-ionized into the hydrogen ions with a number $v_{\text{rec}}\tau_{\text{ion}} = \beta N n_{\text{e}}\alpha_{\text{B}}\tau_{\text{ion}} = \beta N \tau_{\text{ion}}/\tau_{\text{rec}}$, where $n_{\text{e}}\alpha_{\text{B}} = 1/\tau_{\text{rec}}$. Thus, the total continuum radiation pressure force on the cloud due to the above two origins is

$$F_{\text{r}} = \frac{L\sigma_{\text{T}}}{4\pi R^2 c}\beta N + \frac{fL\sigma_{\text{bf}}}{4\pi R^2 c}\beta N \frac{\tau_{\text{ion}}}{\tau_{\text{rec}}}, \quad (3)$$

where $f = L_{\text{ion}}/L$ is the ratio of the ionizing luminosity L_{ion} to the central source luminosity L , σ_{T} is the Thomson cross-section, c is the speed of light, βN is the ionized number of hydrogen atoms in the cloud, σ_{bf} is the flux-weighted average of the hydrogen bound-free

absorption cross-section, and τ_{rec} is the hydrogen ion recombination timescale in the cloud. The two continuum radiation pressure forces in equation (3) are similar to those in equation (9) in Krause et al. (2012) that focused on stability of BLR clouds. The resultant of forces is $F_t = F_G - F_c - F_r$. As $F_t = 0$, we have

$$\begin{aligned} M_{\bullet} &= \frac{v^2 R}{G} + \beta \frac{L \sigma_T}{4\pi c G m_H} + \beta \frac{f L \sigma_{\text{bf}}}{4\pi c G m_H} \frac{\tau_{\text{ion}}}{\tau_{\text{rec}}} \\ &= \frac{v^2 R}{G} + \frac{L \sigma_T}{4\pi c G m_H} \left(\beta + \beta f \frac{\sigma_{\text{bf}}}{\sigma_T} \frac{\tau_{\text{ion}}}{\tau_{\text{rec}}} \right) \\ &= M_{\text{BH}} + 7.95 \times 10^6 \left(\beta + \beta f \frac{\sigma_{\text{bf}}}{\sigma_T} \frac{\tau_{\text{ion}}}{\tau_{\text{rec}}} \right) L_{45} (M_{\odot}) \\ &= M_{\text{BH}} + M_{\text{RP}}, \end{aligned} \tag{4}$$

where $m \approx N m_H$ is used in the deduction, $L_{45} = L/10^{45} \text{ erg s}^{-1}$, M_{BH} is the black hole mass estimated as L is not considered, and M_{RP} is the black hole mass counteracted by the continuum radiation pressure due to the central engine luminosity.

The cross-section σ_{bf} is equal to

$$\sigma_{\text{bf}} = \frac{\int_{\nu_H}^{\infty} F_{\nu} \sigma_{\nu} d\nu}{\int_{\nu_H}^{\infty} F_{\nu} d\nu} = \frac{\int_{\nu_H}^{\infty} F_{\nu} \sigma_{\nu} d\nu}{F_{\text{ion}}} = \frac{\int_{\nu_H}^{\infty} F_{\nu} \sigma_{\nu} d\nu}{f F}, \tag{5}$$

where $F_{\nu} \propto \nu^{-\alpha}$, ν_H is the frequency of 13.6 eV photon, σ_{ν} is the photoionization cross-section of hydrogen, F_{ion} is the ionizing radiation flux, and F is the total radiation flux. For $\alpha = 1.5$ (Tarter & McKee 1973), $\sigma_{\text{bf}} \simeq 1.1 \times 10^{-18} \text{ cm}^2$. The ionizing timescale is

$$\tau_{\text{ion}} = \left(\int_{\nu_H}^{\infty} \frac{F_{\nu} \sigma_{\nu}}{h \nu} d\nu \right)^{-1}. \tag{6}$$

The recombination timescale of ionized hydrogen is

$$\tau_{\text{rec}} = (n_e \alpha_B(T))^{-1}, \tag{7}$$

where $n_e = \beta n_H$ is the free electron number density and n_H is the number density of hydrogen. The hydrogen recombination coefficient $\alpha_B(T)$ was given with a set of formulae

in Seaton (1959). An analytic expression of α_B to the excited levels of hydrogen is given by Hummer & Seaton (1963)

$$\alpha_B(T) = 1.627 \times 10^{-13} T_4^{-1/2} [1 - 1.657 \log T_4 + 0.584 T_4^{1/3}] \text{ cm}^3 \text{ s}^{-1}, \quad (8)$$

where $T_4 = 10^{-4}T$, and T in units of K is the electron temperature of clouds. As $0.5 \leq T_4 \leq 10$, equation (8) gives α_B to an accuracy of better than 1 percent relative to the result of Seaton (1959). The photoionized gas in clouds is at $T \sim 10^4$ K and produces optical and ultraviolet emission lines of quasars (Krolik et al. 1981). Photoionization governs the thermodynamics of the clouds that have a stable equilibrium temperature of order 10^4 K, independent of their locations (Krause et al. 2011). In the case of $T \sim 10^4$ K, $\alpha_B \sim 2.6 \times 10^{-13} \text{ cm}^3 \text{ s}^{-1}$. For the BLRs of AGNs, Bentz et al. (2009a) presented the calibrated radius-luminosity relation

$$\log R = -21.3 + 0.519 \log \lambda L_\lambda(5100\text{\AA}), \quad (9)$$

where R and $\lambda L_\lambda(5100\text{\AA})$ are in units of light days and erg s^{-1} , respectively. The radiation flux $F = L/4\pi R^2$.

In general, there is $0 < \beta < 1$ that means a partially ionized cloud. $\beta = 1$ means a fully ionized cloud, and $\beta = 0$ means a fully non-ionized cloud. First, we consider a case that a fraction of hydrogen is ionized, and we will take $\beta = 0.1$ (Case A). The cloud may be mostly ionized, and we will take $\beta = 0.5$ (Case B). The ratio of L_{ion}/L has an average $f \simeq 0.6$ (Marconi et al. 2008). A typical value of $n_H = 10^{10} \text{ cm}^{-3}$ was obtained for the BLRs of AGNs (Davidson & Netzer 1979; Ferland & Elitzur 1984; Rees et al. 1989). The luminosity L is estimated with $L = 9 \times \lambda L_\lambda(5100\text{\AA})$ (Kaspi et al. 2000). $L = 6 \times \lambda L_\lambda(3000 \text{\AA})$ is used for the ultraviolet (UV) continuum (e.g. Willott et al. 2010). The range of $0 < \beta < 1$ is suggested by the corresponding variations between the broad-line and continuum light curves in the reverberation mapping observations (e.g. Kaspi & Netzer

1999; Kaspi et al. 2000, 2005). In the following section, we take $f = 0.6$, $n_{\text{H}} = 10^{10} \text{ cm}^{-3}$, $T = 10^4 \text{ K}$, and $\alpha = 1.5$ to estimate M_{RP} for Cases A and B.

3. APPLICATIONS

We collect 40 high accretion rate AGNs, including quasars and broad-line Seyfert 1 galaxies, with the black hole virial masses M_{RM} estimated from the reverberation mapping method (see Table 1). Table 1 consists of four parts. The first part contains 17 AGNs, collected from Peterson et al. (2004), with relatively high accretion rates. The second part contains 13 AGNs with super-Eddington accreting massive black holes (SEAMBHs, Du et al. 2015). The first results from a new reverberation mapping campaign are reported in Du et al. (2014) for the SEAMBH AGNs. The new reverberation mapping observations of the SEAMBH AGNs are presented in Wang et al. (2014a) and Hu et al. (2015). The third part contains 9 quasars in the Canada-France High- z Quasar Survey (CFHQS) at redshift $z \gtrsim 6$, accreting close to the Eddington limit (Willott et al. 2010). The last one contains 2 AGNs from other works. There is one overlap AGN (see Table 1). The CFHQS quasars have M_{RM} and luminosity $\lambda L_{\lambda}(3000 \text{ \AA})$. The optical luminosity $\lambda L_{\lambda}(\text{opt})$ around 5100 \AA at the rest frame of source is used to estimate L with $L = 9 \times \lambda L_{\lambda}(\text{opt})$ (Kaspi et al. 2000). As in Willott et al. (2010), $L = 6 \times \lambda L_{\lambda}(3000 \text{ \AA})$ is used for the CFHQS quasars. The estimated results of M_{RP} are presented in Table 1.

Figure 1 shows the comparisons of M_{RP} to M_{RM} . For Case A, four AGNs with SEAMBHs and three CFHQS quasars have $M_{\text{RP}} \gtrsim 0.5 M_{\text{RM}}$ (see Figure 1a and Table 1). For Case A, 9 AGNs match $M_{\text{RP}} \gtrsim 0.3 M_{\text{RM}}$ (see Figure 1a). For Case B, all AGNs match $M_{\text{RP}} \gtrsim 0.5 M_{\text{RM}}$, and 30 AGNs follow $M_{\text{RP}} \gtrsim M_{\text{RM}}$ (see Figure 1b). These comparisons show that the continuum radiation pressures of the central engines have a significant influence on the black hole virial mass estimates on the basis of the reverberation mapping

method. The masses M_{RP} are sensitive to the percent of ionized hydrogen atoms β in the clouds. For some AGNs, such as IRAS F12397, IRAS 04416, and J1641+3755, the continuum radiation pressures can counteract about 30–40 percent gravitational forces of M_{\bullet} (Case A).

In the plots of M_{RP} versus M_{RM} , the SEAMBH AGNs, the CFHQS quasars, and the rest of AGNs populate in the narrow zones (see Figure 1). From this view point, the SEAMBH AGNs at $z < 0.2$ and the CFHQS quasars at $z \gtrsim 6$ are not essentially different. This means that their central black holes are likely accreting at the very high rates, regardless of the environments surrounding these AGNs, but maybe related to the environments surrounding the central black holes, such as dusty tori and accretion disks. Also, some of the rest of AGNs are at the similar accretion rates to those of the SEAMBH AGNs and the CFHQS quasars. Whether or not the continuum radiation pressure is considered to estimate M_{\bullet} depends on the ratio of $M_{\text{RP}}/M_{\text{RM}}$. The radiation pressure must be considered as $M_{\text{RP}}/M_{\text{RM}} \gtrsim 0.5$ that will lead to underestimate M_{\bullet} by a factor $\gtrsim 1/3$, i.e., $M_{\bullet} \gtrsim 1.5M_{\text{RM}}$. When $M_{\text{RP}}/M_{\text{RM}} \gtrsim 1.0$, M_{\bullet} will be underestimated by a factor $\gtrsim 1/2$, i.e., $M_{\bullet} \gtrsim 2.0M_{\text{RM}}$. Thus, the importance of the continuum radiation pressure can not be neglected in estimating M_{\bullet} for the high accretion rate AGNs.

4. DISCUSSION AND CONCLUSIONS

There is a undetermined parameter β , the ionization percent of the BLR clouds, in equations (3) and (4). Two values of $\beta = 0.1$ and $\beta = 0.5$ are assumed to estimate M_{RP} . These assumptions may lead to some unreasonable results. Following the Strömgren radius of a Strömgren sphere of ionized hydrogen around a young star (Strömgren 1939), an ionization depth of a cloud is defined as the position where the recombination rate equals the ionization rate, and the hydrogen atoms are fully ionized. As the recombination

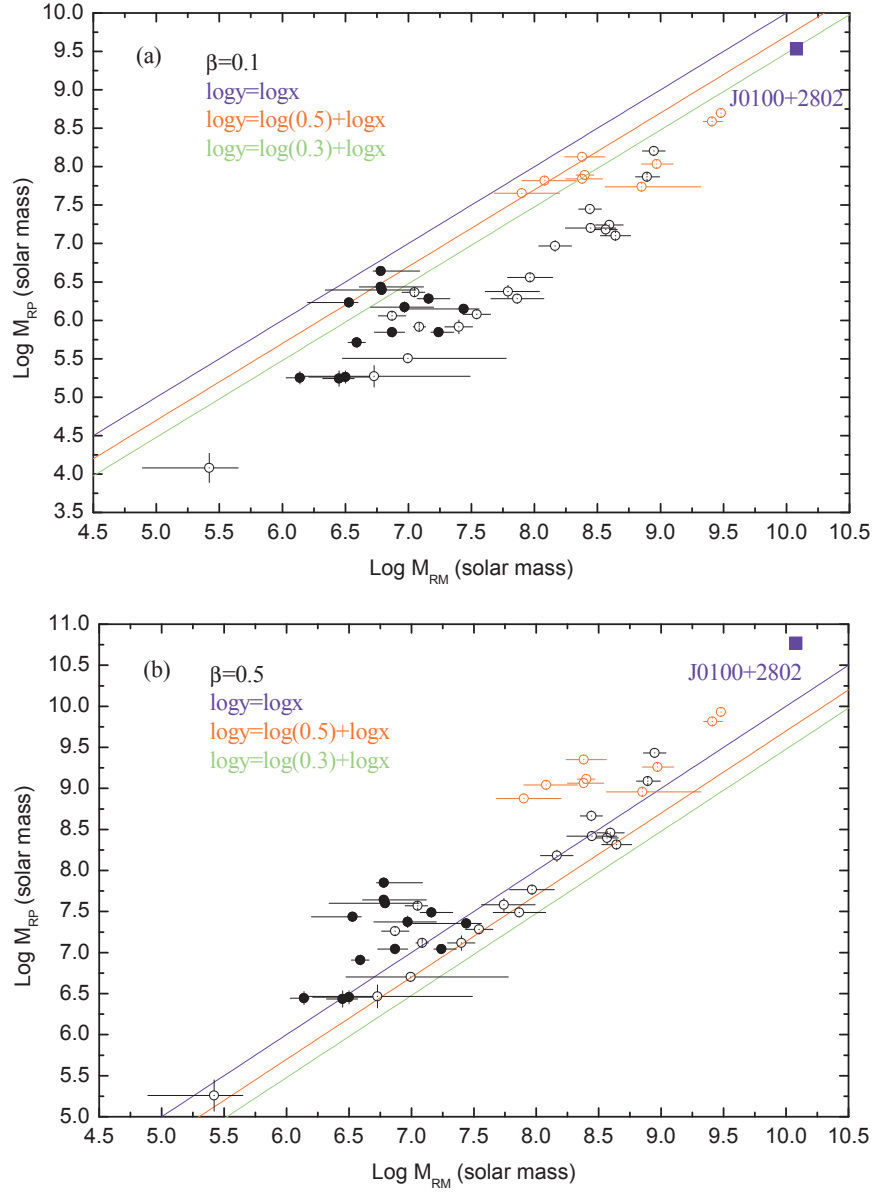


Fig. 1.— Black hole masses counteracted by radiation pressures versus black hole masses estimated with the reverberation mapping method. Solid lines in plots (a) and (b) correspond to the different ratios of y/x . Solid black circles correspond to the AGNs with SEAMBHs (Du et al. 2015). Red open circles are the CFHQS quasars at $z \sim 6$ (Willott et al. 2010). Black open circles are the rest of AGNs in Table 1.

and ionization are in equilibrium, the ionizing photon number arriving at one cloud per unit time equals the recombination line photon number per unit time. The ionizing photon number arriving at the cloud per unit time is $A_c Q(H)/4\pi R^2 = A_c U c n_H$, where A_c is the cross-section area of the cloud, $Q(H) = L_{\text{ion}}/\langle h\nu \rangle$ is the ionizing photon number emitted by the central engine per unit time ($\langle h\nu \rangle$ the mean energy of photons), $U = Q(H)/4\pi R^2 c n_H$ is the ionization parameter of hydrogen, and n_H is the hydrogen number density of the cloud. At the same time, the ionized region of the cloud produces the recombination line photon number per unit time $n_e n_H \alpha_B V_{\text{c,ion}}$, where n_e is the electron number density in this region, and $V_{\text{c,ion}}$ is the fully ionized volume of the cloud. Thus, we have $A_c U c n_H = n_e n_H \alpha_B V_{\text{c,ion}}$ because of the ionization balance. The ionization depth of the cloud is $D_{\text{ion}} \simeq V_{\text{c,ion}}/A_c = Uc/n_e \alpha_B = Uc/n_H \alpha_B$. The cloud has $\beta = V_{\text{c,ion}}/V_c \simeq D_{\text{ion}}/D_c$, where V_c and D_c are the volume and thickness of the cloud, respectively.

The ionization parameter has $U \sim 0.1$ – 1 for emission line gas in quasars and Seyfert galaxies (Davidson 1972; McKee & Tarter 1975; Kwan & Krolik 1981). A gas density of 10^9 – 10^{10} cm^{-3} is required by a very large Lyman continuum optical depth (e.g. Krolik et al. 1981). The gas density values are the same as those in Kwan & Krolik (1981) for quasars and Seyfert galaxies. Ferland & Elitzur (1984) got $n_H = 10^{10 \pm 1} \text{ cm}^{-3}$. A density of $10^9 \lesssim n_H \lesssim 10^{11} \text{ cm}^{-3}$ is set by the presence of broad semi-forbidden line C III] λ 1909 and the absence of broad forbidden lines such as [O III] $\lambda\lambda$ 4363, 4959, 5007 (Davidson & Netzer 1979; Rees et al. 1989). The typical values are $n_H \sim 10^{10} \text{ cm}^{-3}$ and $U \sim 0.1$ (e.g. Rees et al. 1989; Laor et al. 2006). The cloud size of $r_c \lesssim (1\text{--}3) \times 10^{12} \text{ cm}$ was constrained by the smoothness of the emission-line profiles (Laor et al. 2006). Baskin et al. (2014) showed a universal ionization parameter $U \sim 0.1$ in the inner photoionized layer of the BLR clouds, independent of luminosity and distance. The radiation pressure confinement of the photoionized layer appears to explain the universality of the BLR properties in AGNs, the similar relative line strength over the vast range of 10^{39} – $10^{47} \text{ erg s}^{-1}$ in luminosity

(Baskin et al. 2014). A widely accepted power-law relation has been established between the luminosity $\lambda L_\lambda(opt)$ and the BLR size R , as $R \propto \lambda L_\lambda^{0.5}(opt)$ (Bentz et al. 2006, 2009a,b; Denney et al. 2010; Kaspi et al. 1996, 2000, 2005, 2007; Greene et al. 2010; Wang & Zhang 2003). This power-law relation spans over a range of 10^7 in $\lambda L_\lambda(opt)$ (Kaspi et al. 2007). Thus, $U = L_{ion}/4\pi R^2 c n_H \langle h\nu \rangle \propto \lambda L_\lambda(opt)/R^2 n_H$. So, U will be independent of $\lambda L_\lambda(opt)$, L_{ion} , and R . This independence may lead to a universal ionization parameter as suggested in Baskin et al. (2014).

The typical values of $n_H \sim 10^{10} \text{ cm}^{-3}$ and $U \sim 0.1$ are taken to estimate D_{ion} , and then β with $\alpha_B \sim 2.6 \times 10^{-13} \text{ cm}^3 \text{ s}^{-1}$ and $D_c \sim 2r_c \lesssim (2-6) \times 10^{12} \text{ cm}$. We have $D_{ion} \sim 1.2 \times 10^{12} \text{ cm}$, and then $\beta \simeq D_{ion}/D_c \gtrsim 0.2-0.6$. Thus, it is basically reasonable to take $\beta = 0.1$ and 0.5 in the calculations of M_{RP} . So, the masses counteracted by the continuum radiation pressures of the central engines are not negligible compared to, or are comparable to the black hole virial masses at least for some AGNs (see Figure 1). This counteracting effect of the continuum radiation pressure is significant for quasars at $z \gtrsim 6$ (see Figure 1). J0100+2802 at $z = 6.30$ has a bolometric luminosity of $L = 1.62 \times 10^{48} \text{ erg s}^{-1}$ and a black hole mass of $\sim 1.2 \times 10^{10} M_\odot$, and it is the most luminous quasar known at $z > 6$ (Wu et al. 2015). It has a $M_{RP} \sim 1.1 \times 10^{9.5} M_\odot$ as $\beta = 0.1$ and $M_{RP} \sim 5.9 \times 10^{10} M_\odot$ as $\beta = 0.5$. These M_{RP} for this object are comparable to the black hole virial mass $\sim 1.2 \times 10^{10} M_\odot$. So, J0100+2802 will have $M_\bullet > 1.2 \times 10^{10} M_\odot$. This larger black hole mass further gives rise to the most significant challenge to the Eddington limit growth of black holes in the early Universe (Volonteri 2012; Willott et al. 2010). There are the same cases for the CFHQS quasars as in J0100+2802 (see Figure 1). Their masses M_\bullet are larger than the virial masses M_{RM} . Wang et al. (2010) suggested for $z \simeq 6$ quasars that the supermassive black holes in the early Universe likely grew much more quickly than their host galaxies. The larger black hole masses M_\bullet of the quasars at $z \gtrsim 6$ further strengthen this suggestion. Thus, it is important to consider the radiation pressure effect on the black

hole mass estimates for the AGNs with the high accretion rates. This importance of the radiation pressure is consistent with that suggested by Marconi et al. (2008) who argued for narrow-line Seyfert 1 galaxies, and seems to be inconsistent with the suggestions in Netzer (2009) and Netzer & Marziani (2010).

An assumption of isotropy in equations (3) and (4) is made for the central source luminosity L . This assumption might significantly influence the estimated values of M_{RP} , and then the results of this paper. The anisotropic illumination of a BLR by the central radiation was discussed by Netzer (1987), and recently was investigated by Wang et al. (2014b). The central radiation of quasars are anisotropic (e.g. Nemmen & Brotherton 2010). Nemmen & Brotherton (2010) derived bolometric corrections based on the theoretical accretion disk models of Hubeny et al. (2000), and obtained an anisotropic correction factor of $f_{\text{ani}} \approx 0.8$, where $f_{\text{ani}} = L/L_{\text{iso}}$ and L_{iso} is the total source luminosity assuming isotropy. Runnoe et al. (2012) got a factor of $f_{\text{ani}} \approx 0.75$ for quasars. So, we take $f_{\text{ani}} = 0.8$, i.e., $L = 0.8L_{\text{iso}}$ to re-estimate M_{RP} , and the re-estimated M_{RP} are compared to M_{RM} in Figure 2. Considering the anisotropy of the central source luminosity L , the continuum radiation pressure effects on the black hole masses M_{\bullet} can not be still neglected for the close- and super-Eddington limit accretion rate AGNs. Thus, the anisotropy of the central source luminosity could not influence significantly the main results assuming isotropy. Wang et al. (2014a) proposed the SEAMBH AGNs as the most luminous standard candles in the Universe. Since a part of the SEAMBH AGNs and the CFHQS quasars have the same behaviors in the plots of M_{RP} versus M_{RM} , the CFHQS quasars likely have the potential to be the most luminous standard candles in the Universe. This potential will extend the redshifts of the most luminous standard candles from $z < 0.2$ up to $z \gtrsim 6$, and will be important to study the Universe because of extending significantly the cosmic distance beyond the range explored by type Ia supernovae (Riess et al. 1998; Perlmutter et al. 1999).

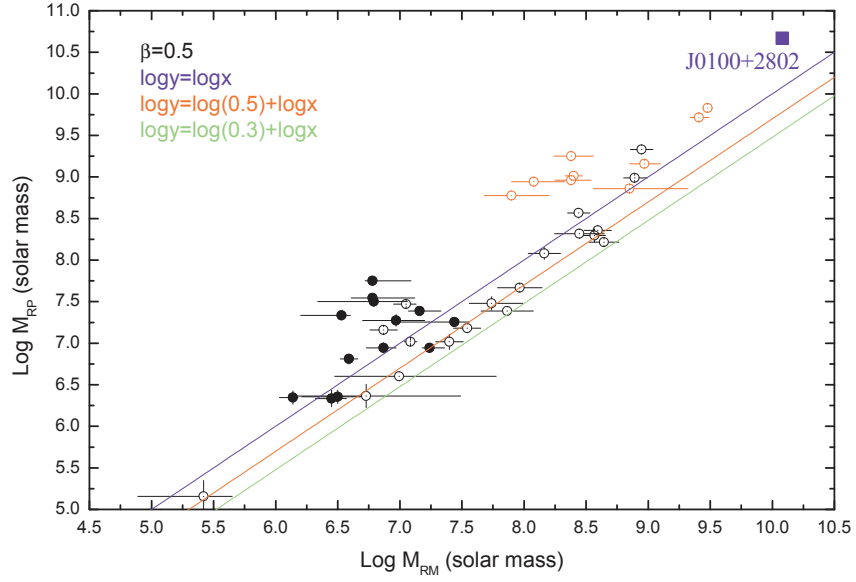


Fig. 2.— M_{RP} versus M_{RM} for the same sources as in Figure 1. The symbols and lines are the same as in Figure 1. M_{RP} are estimated as considering the anisotropy of the central engine luminosity L .

An average column density of a cloud is $N_{\text{H}} \sim 10^{22} \text{ cm}^{-2}$ ($n_{\text{H}} \sim 10^{10} \text{ cm}^{-3}$ and $D_{\text{c}} \sim (2\text{--}6) \times 10^{12} \text{ cm}$). The electron Thomson scattering optical depth of the cloud is $N_{\text{H}}\sigma_{\text{T}} \sim 10^{-2} \ll 1$, and the cloud is optically thin, which confirms the fourth assumption of the model. The ionizing optical depth of the cloud is $N_{\text{H}}\sigma_{\text{bf}} \sim 10^4 \gg 1$, and the cloud is optically thick to the ionizing photons. The cloud has the Strömgren radius smaller than its thickness. So, the cloud is partially ionized, confirming the first assumption of the model, and this is consistent with the constraints set by the reverberation mapping observations. The radiation pressure force ratio of the second to the first term in equation (3) has averages $\simeq 1.2\text{--}6.3$ for AGNs in Table 1. The first term of the free electron Thomson scattering is comparable to the second term of the recombination and re-ionization of the hydrogen ions. The second term becomes more important as β increases. The partly ionized clouds will be ionized more as L_{ion} increases, and the second term would be more important as the central engines become brighter. The radiation pressure forces due to absorption of ionizing photons and Thomson scattering were used to modify the expression for the black hole virial mass M_{RM} (see equation 5 in Marconi et al. 2008). As $N_{\text{H}} \sim 10^{22}\text{--}10^{23} \text{ cm}^{-2}$, the modified M_{RM} becomes larger by a factor of $\sim 10\text{--}100$ for the AGNs accreting around the Eddington limit. In consequence, J0100+2802 at $z = 6.30$ will have $M_{\bullet} \sim 10^{11}\text{--}10^{12} M_{\odot}$ that is nearly impossible to the Eddington limit growth of black holes in the early Universe because of the larger initial masses of primary black holes. If considering the line-driven radiation pressure force (Castor et al. 1975), the radiation pressure force due to the gas opacity will be $\sim 10^3$ times that due to the electron scattering opacity (Ferland et al. 2009). This will bring a larger mass $M_{\bullet} \sim M_{\text{RP}} \sim 10^{12}\text{--}10^{13} M_{\odot}$ for J0100+2802. These extremely large corrected masses of the black hole in J0100+2802 indicate some problem of their treatments of the radiation pressure forces on the BLR clouds in AGNs, or the model of formation and evolution of black hole, or the model of the Universe.

In this paper, we investigate the influences of two continuum radiation pressures,

usually believed negligible or not considered, of the central engines in AGNs on the black hole mass estimates with the reverberation mapping method or the descendent methods. The continuum radiation pressure forces are from two origins: the free electron Thomson scattering of the central radiation, and the recombination and re-ionization of the ionized hydrogen. The radiation pressures depend on a parameter β , the ionized percent of the clouds in a BLR. The counteracted black hole masses by the radiation pressures M_{RP} are compared to the black hole virial masses M_{RM} for 40 AGNs with the high accretion rates. The masses M_{RP} are sensitive to β . As $\beta = 0.5$, $M_{\text{RP}} \gtrsim 0.3M_{\text{RM}}$ for all the AGNs in Figure 2. As $\beta = 0.1$, the radiation pressures can counteract at least about 30–40 percent gravitational forces of the black holes for some AGNs (see Figure 1). Four SEAMBH AGNs at $z < 0.2$ and five CFHQS quasars at $z \gtrsim 6.0$ are around the line $M_{\text{RP}} = 0.5M_{\text{RM}}$ for $\beta = 0.1$ (see Figure 1a). Thus, the continuum radiation pressures of the central engines have to be considered in estimating the black hole masses for the AGNs accreting around the Eddington limit, regardless of the redshifts or the surrounding environments of AGNs. The most luminous quasar J0100+2802 likely has the same case as the nine AGNs (see Figures 1 and 2). A part of the SEAMBH AGNs and the CFHQS quasars is blended with the non-SEAMBH and non-CFHQS AGNs (see Figures 1 and 2). The close- and super-Eddington limit accreting AGNs are not different from the rest of AGNs. The anisotropy of the central source luminosity could not influence significantly the main results assuming isotropy. The force multiplier, the ratio of gas opacity to electron scattering opacity (Castor et al. 1975; Ferland et al. 2009), will be needed for the AGNs with $M_{\text{RP}} \gtrsim 0.3M_{\text{RM}}$ due to the radiation pressures in equation (3). Though, some extremely large masses are derived from the force multiplier $\sim 10^3$ for the black hole in J0100+2802 ($M_{\text{RP}} \sim 10^{12}\text{--}10^{13} M_{\odot}$). In future, the force multiplier, due to the photoionization absorption, and the resonance and subordinate line absorption, could be calculated with the spectral simulation code Cloudy described by Ferland et al. (1998),

and with detailed parameters of the BLR structure, the cloud distribution, the gas density of cloud, the chemical abundances of gas, the central continuum, and the observed emission lines, for each high accretion rate AGNs.

H.T.L. thanks the National Natural Science Foundation of China (NSFC; grants 11273052 and U1431228) for financial support. J.M.B. acknowledges the support of the NSFC (grant 11133006). H.T.L. thanks the financial supports of the Youth Innovation Promotion Association, CAS and the project of the Training Programme for the Talents of West Light Foundation, CAS.

REFERENCES

- Baskin, A., Laor, A., & Stern, J. 2014, MNRAS, 438, 604
- Bentz, M. C., Denney, K. D., Cackett, E. M., et al. 2007, ApJ, 662, 205
- Bentz, M. C., Denney, K. D., Grier, C. J., et al. 2013, ApJ, 767, 149
- Bentz, M. C., Peterson, B. M., Pogge, R. W., et al. 2006, ApJ, 644, 133
- Bentz, M. C., Peterson, B. M., Netzer, H., Pogge, R. W., & Vestergaard, M. 2009a, ApJ, 697, 160
- Bentz, M. C., Walsh, J. L., Barth, A. J., et al. 2009b, ApJ, 705, 199
- Blandford, R. D., & McKee, C. F. 1982, ApJ, 255, 419
- Castor, J. I., Abbott, D. C., & Klein, R. I. 1975, ApJ, 195, 157
- Davidson, K. 1972, ApJ, 171, 213
- Davidson, K., & Netzer, H. 1979, Rev. Mod. Phys., 51, 715
- Denney, K. D., Peterson, B. M., Pogge, R. W., et al. 2010, ApJ, 721, 715
- Du, P., Hu, C., Lu, K. X., et al. (SEAMBH Collaboration) 2014, ApJ, 782, 45
- Du, P., Hu, C., Lu, K. X., et al. (SEAMBH Collaboration) 2015, ApJ, 806, 22
- Ferland, G. J., & Elitzur, M. 1984, ApJ, 285, L11
- Ferland, G. J., Hu, C., Wang, J. M., et al. 2009, ApJL, 707, L82
- Ferland, G. J., Korista, K. T., Verner, D. A., et al. 1998, PASP, 110, 761
- Gaskell, C. M. 2009, NewAR, 53, 140

- Greene, J. E., Hood, C. E., Barth, A. J., et al. 2010, *ApJ*, 723, 409
- Grier, C. J., Peterson, B. M., Pogge, R. W., et al. 2012, *ApJ*, 755, 60
- Hu, C., Du, P., Lu, K. X., et al. (SEAMBH Collaboration) 2015, *ApJ*, 804, 138
- Hubeny, I., Agol, E., Blaes, O., & Krolik, J. H., 2000, *ApJ*, 533, 710
- Hummer, D. G., & Seaton, M. J. 1963, *MNRAS*, 125, 437
- Kaspi, S., Brandt, W. N., Maoz, D., et al. 2007, *ApJ*, 659, 997
- Kaspi, S., Maoz, D., Netzer, H., et al. 2005, *ApJ*, 629, 61
- Kaspi, S., & Netzer, H. 1999, *ApJ*, 524, 71
- Kaspi, S., Smith, P. S., Maoz, D., et al. 1996, *ApJL*, 471, 75
- Kaspi, S., Smith, P. S., Netzer, H., et al. 2000, *ApJ*, 533, 631
- Krause, M., Burkert, A., & Schartmann, M. 2011, *MNRAS*, 411, 550
- Krause, M., Schartmann, M., & Burkert, A. 2012, *MNRAS*, 425, 3172
- Krolik, J. H., McKee, C. F., & Tarter, C. B. 1981, *ApJ*, 249, 422
- Kwan, J., & Krolik, J. H. 1981, *ApJ*, 250, 478
- Laor, A., Barth, A. J., Ho, L. C., & Filippenko, A. V. 2006, *ApJ*, 636, 83
- Marconi, A., Axon, D. J., Maiolino, R., et al. 2008, *ApJ*, 678, 693
- Marconi, A., Axon, D. J., Maiolino, R., et al. 2009, *ApJ*, 698, L103
- McKee, C. F., & Tarter, C. B. 1975, *ApJ*, 202, 306
- Nemmen, R. S., & Brotherton, M. S. 2010, *MNRAS*, 408, 1598

- Netzer, H. 1987, MNRAS, 225, 55
- Netzer, H. 2009, ApJ, 695, 793
- Netzer, H., & Marziani, P. 2010, ApJ, 724, 318
- Peterson, B. M. 1993, PASP, 105, 247
- Peterson, B. M., Ferrarese, L., Gilbert, K. M., et al. 2004, ApJ, 613, 682
- Peterson, B. M., Bentz, M. C., Desroches, L. B., et al. 2005, ApJ, 632, 799
- Peterson, B. M., & Wandel, A. 1999, ApJ, 521, L95
- Perlmutter, S., Aldering, G., Goldhaber, G., et al. 1999, ApJ, 517, 565
- Rees, M. J. 1984, ARA&A, 22, 471
- Rees, M. J., Begelman, M. C., Blandford, R. D., & Phinney, E. S. 1982, Natur, 295, 17
- Rees, M. J., Netzer, H., & Ferland, G. J. 1989, ApJ, 347, 640
- Riess, A. G., Filippenko, A. V., Challis, P., et al. 1998, AJ, 116, 1009
- Runnoe, J., C., Brotherton, M., S., & Shang, Z. 2012, MNRAS, 422, 478
- Seaton, M. J. 1959, MNRAS, 119, 81
- Strömgren, B. 1939, ApJ, 89, 526
- Tarter, C. B., & McKee, C. F. 1973, ApJL, 186, L63
- Ulrich, M. H., Maraschi, L., & Urry, C. M. 1997, ARA&A, 35, 445
- Volonteri, M. 2012, Science, 337, 544
- Wang, J. M., Du, P., Hu, C., et al. (SEAMBH Collaboration) 2014a, ApJ, 793, 108

Wang, J. M., Qiu, J., Du, P., & Ho, L. C. 2014b, *ApJ*, 797, 65

Wang, R., Carilli, C., L., Neri, R., et al. 2010, *ApJ*, 714, 699

Wang, T. G., & Zhang, X. G. 2003, *MNRAS*, 340, 793

Willott, C. J., Albert, L., Arzoumanian, D., et al. 2010, *AJ*, 140, 546

Wu, X. B., Wang, F., Fan, X., et al. 2015, *Natur*, 518, 512

Table 1. Sample of AGNs with the virial black hole masses

Name	z	$\log \frac{\lambda L_{\lambda}(opt)}{\text{erg s}^{-1}}$	$\log \frac{M_{\text{RM}}}{M_{\odot}}$	Refs.	$\log \frac{M_{\text{RP}}}{M_{\odot}}$	$\log \frac{M_{\text{BP}}}{M_{\odot}}$
(1)	(2)	(3)	(4)	(5)	(6)	(7)
Mrk 335	0.026	43.86 ± 0.04	7.15 ± 0.11	1	6.06 ± 0.04	7.26 ± 0.04
PG 0026+129	0.142	45.02 ± 0.06	8.59 ± 0.11	1	7.24 ± 0.06	8.46 ± 0.06
PG 0052+251	0.155	44.96 ± 0.08	8.57 ± 0.09	1	7.18 ± 0.08	8.40 ± 0.08
3C 120	0.033	44.17 ± 0.08	$7.74^{+0.25}_{-0.18}$	1	6.37 ± 0.08	7.58 ± 0.08
PG 0844+349	0.064	44.35 ± 0.04	7.97 ± 0.18	1	6.56 ± 0.04	7.77 ± 0.04
Mrk 110	0.035	43.72 ± 0.09	7.40 ± 0.11	1	5.92 ± 0.09	7.12 ± 0.09
PG 0953+414	0.234	45.22 ± 0.06	8.44 ± 0.09	1	7.45 ± 0.06	8.67 ± 0.06
PG 1211+143	0.081	44.75 ± 0.07	8.16 ± 0.13	1	6.97 ± 0.07	8.18 ± 0.07
PG 1226+023	0.158	45.96 ± 0.05	8.95 ± 0.09	1	8.20 ± 0.05	9.43 ± 0.05
PG 1229+204	0.063	44.08 ± 0.05	7.86 ± 0.21	1	6.28 ± 0.05	7.49 ± 0.05
NGC 4593	0.009	43.09 ± 0.14	$6.73^{+0.76}_{-0.56}$	1	5.27 ± 0.14	6.47 ± 0.14
PG 1307+085	0.155	44.88 ± 0.04	8.64 ± 0.12	1	7.10 ± 0.04	8.31 ± 0.04
IC 4329A	0.016	43.32 ± 0.05	$7.00^{+0.78}_{-0.52}$	1	5.51 ± 0.05	6.70 ± 0.05
Mrk 279	0.030	43.88 ± 0.05	7.54 ± 0.11	1	6.08 ± 0.05	7.28 ± 0.05
PG 1613+658	0.129	44.98 ± 0.05	8.45 ± 0.20	1	7.20 ± 0.05	8.42 ± 0.05
PG 1700+518	0.292	45.63 ± 0.03	$8.89^{+0.10}_{-0.09}$	1	7.87 ± 0.03	9.09 ± 0.03
NGC 7469	0.016	43.72 ± 0.02	7.09 ± 0.05	1	5.92 ± 0.02	7.12 ± 0.02
*Mrk 335	0.026	43.65 ± 0.06	$6.87^{+0.10}_{-0.14}$	2	5.84 ± 0.06	7.04 ± 0.06
Mrk 1044	0.017	43.06 ± 0.10	$6.45^{+0.12}_{-0.13}$	2	5.24 ± 0.10	6.43 ± 0.10
Mrk 382	0.034	43.08 ± 0.08	$6.50^{+0.19}_{-0.29}$	2	5.26 ± 0.08	6.46 ± 0.08
Mrk 142	0.045	43.52 ± 0.06	$6.59^{+0.07}_{-0.07}$	2	5.71 ± 0.06	6.91 ± 0.06
IRAS F12397	0.043	44.19 ± 0.05	$6.79^{+0.27}_{-0.45}$	2	6.40 ± 0.05	7.60 ± 0.05
Mrk 486	0.039	43.65 ± 0.05	$7.24^{+0.12}_{-0.06}$	2	5.84 ± 0.05	7.04 ± 0.05
Mrk 493	0.031	43.07 ± 0.08	$6.14^{+0.04}_{-0.11}$	2	5.25 ± 0.08	6.45 ± 0.08
IRAS 04416	0.089	44.43 ± 0.03	$6.78^{+0.31}_{-0.06}$	2	6.64 ± 0.03	7.85 ± 0.03
SDSS J075101	0.121	44.08 ± 0.05	$7.16^{+0.17}_{-0.09}$	2	6.28 ± 0.05	7.49 ± 0.05
SDSS J080101	0.140	44.23 ± 0.03	$6.78^{+0.34}_{-0.17}$	2	6.44 ± 0.03	7.64 ± 0.03
SDSS J081441	0.163	43.97 ± 0.07	$6.97^{+0.23}_{-0.27}$	2	6.17 ± 0.07	7.37 ± 0.07
SDSS J081456	0.120	43.95 ± 0.04	$7.44^{+0.12}_{-0.49}$	2	6.15 ± 0.04	7.35 ± 0.04
SDSS J093922	0.186	44.03 ± 0.04	$6.53^{+0.07}_{-0.33}$	2	6.23 ± 0.04	7.44 ± 0.04
J0210-0456	6.438	$45.60 \pm 0.05^{\dagger}$	$7.90^{+0.30}_{-0.22}$	3	7.66 ± 0.05	8.88 ± 0.05

Table 1—Continued

Name	z	$\log \frac{\lambda L_{\lambda}(opt)}{\text{erg s}^{-1}}$	$\log \frac{M_{RM}}{M_{\odot}}$	Refs.	$\log \frac{M_{RP}}{M_{\odot}}$	$\log \frac{M_{RP}}{M_{\odot}}$
(1)	(2)	(3)	(4)	(5)	(6)	(7)
J2329-0301	6.417	$45.83 \pm 0.05^{\dagger}$	$8.40^{+0.07}_{-0.07}$	3	7.89 ± 0.05	9.11 ± 0.05
J0050+3445	6.253	$46.51 \pm 0.04^{\dagger}$	$9.41^{+0.08}_{-0.07}$	3	8.59 ± 0.04	9.82 ± 0.04
J0221-0802	6.161	$45.68 \pm 0.04^{\dagger}$	$8.85^{+0.47}_{-0.29}$	3	7.74 ± 0.04	8.96 ± 0.04
J2229+1457	6.152	$45.76 \pm 0.04^{\dagger}$	$8.08^{+0.25}_{-0.18}$	3	7.82 ± 0.04	9.04 ± 0.04
J1509-1749	6.121	$46.62 \pm 0.04^{\dagger}$	$9.48^{+0.04}_{-0.04}$	3	8.70 ± 0.04	9.93 ± 0.04
J2100-1715	6.087	$45.97 \pm 0.04^{\dagger}$	$8.97^{+0.13}_{-0.12}$	3	8.03 ± 0.04	9.26 ± 0.04
J1641+3755	6.047	$46.06 \pm 0.05^{\dagger}$	$8.38^{+0.18}_{-0.14}$	3	8.13 ± 0.05	9.35 ± 0.05
J0055+0146	5.983	$45.78 \pm 0.05^{\dagger}$	$8.38^{+0.16}_{-0.13}$	3	7.84 ± 0.05	9.06 ± 0.05
NGC 4051	0.002	41.92 ± 0.19	$5.42^{+0.23}_{-0.53}$	2,4,5	4.08 ± 0.19	5.26 ± 0.19
PG 2130+099	0.063	44.16 ± 0.03	$7.05^{+0.08}_{-0.10}$	2,4,6	6.36 ± 0.03	7.57 ± 0.03

Note. — Column 1: AGN names; Column 2: redshifts of objects; Column 3: Optical luminosity mainly around 5100 Å at rest frame; Column 4: the black hole masses estimated from the reverberation mapping observations; Column 5: the references for columns 3 and 4; Column 6: the black hole masses counteracted by the continuum radiation pressure as $\beta = 0.1$; Column 7: the black hole masses counteracted by the radiation pressure as $\beta = 0.5$; The sign * denotes the other measured results for the same source as in the first part of Table 1. The sign † denotes the UV luminosity around 3000 Å at the rest frame of source. **References:** (1) Peterson et al. 2004, (2) Du et al. 2015, (3) Willott et al. 2010, (4) Bentz et al. 2013, (5) Denney et al. 2010, (6) Grier et al. 2012.